USGS
science for a changing world

Seismic Techniques and Suggested Instrumentation to Monitor Volcanoes

Chapter B of
Recommended Capabilities and Instrumentation for Volcano Monitoring in the United States

Scientific Investigations Report 2024–5062

U.S. Department of the Interior
U.S. Geological Survey

Cover. Multidisciplinary monitoring site Sugar Bowl at Mount St. Helens, Washington. The steaming 2004–2008 volcanic dome is visible in the background. Photograph by T. Paladino, U.S. Geological Survey, February 13, 2024. Background image shows a typical view of the 2008–2018 lava lake in the Overlook crater within Halemaʻumaʻu, Kīlauea. Photograph taken from a helicopter by Tim Orr, U.S. Geological Survey, on August 16, 2013.

Seismic Techniques and Suggested Instrumentation to Monitor Volcanoes

By Weston A. Thelen, John J. Lyons, Aaron G. Wech, Seth C. Moran, Matthew M. Haney, and Ashton F. Flinders

Chapter B of
Recommended Capabilities and Instrumentation for Volcano Monitoring in the United States

Edited by Ashton F. Flinders, Jacob B. Lowenstern, Michelle L. Coombs, and Michael P. Poland

Scientific Investigations Report 2024–5062

U.S. Department of the Interior
U.S. Geological Survey

U.S. Geological Survey, Reston, Virginia: 2024

Suggested citation:
Thelen, W.A., Lyons, J.J., Wech, A.G., Moran, S.C., Haney, M.M., and Flinders, A.F., 2024, Seismic techniques and suggested instrumentation to monitor volcanoes, chap. B *of* Flinders, A.F., Lowenstern, J.B., Coombs, M.L., and Poland, M.P., eds., Recommended capabilities and instrumentation for volcano monitoring in the United States: U.S. Geological Survey Scientific Investigations Report 2024–5062–B, 9 p., https://doi.org/10.3133/sir20245062B.

ISSN 2328-031X (print)
ISSN 2328-0328 (online)

Contents

Figures

Conversion Factors

International System of Units to U.S. customary units

Multiply	By	To obtain
	Length	
meter (m)	3.281	foot (ft)
meter (m)	1.094	yard (yd)
kilometer (km)	0.6214	mile (mi)

Abbreviations

ANSS Advanced National Seismic System

GNSS Global Navigation Satellite System

M magnitude

VLP very long period

Chapter B

Seismic Techniques and Suggested Instrumentation to Monitor Volcanoes

By Weston A. Thelen, John J. Lyons, Aaron G. Wech, Seth C. Moran, Matthew M. Haney, and Ashton F. Flinders

Introduction

Changes in the pressure or location of magma can stress or break surrounding rocks and trigger flow of nearby waters and gases, causing seismic signals, such as discrete earthquakes and tremor. These phenomena are types of seismic unrest that commonly precede eruption and can be used to forecast volcanic activity. Mass movements at the surface, including avalanches, debris flows, and lahars, may also generate seismic signals that are specifically addressed in chapter H, this volume (Thelen and others, 2024). Our focus in this chapter is to determine the levels of instrumentation recommended to produce high-quality, well-constrained seismic observations important for early warning of impending eruptions, detecting changes in ongoing eruptions, and characterizing other hazardous volcanic events.

There are emerging techniques and new types of instrumentation, such as distributed acoustic sensing or rotational seismometers, that we do not consider here. These types of instrumentation show promise for monitoring but still require maturation before being considered more generally in volcano monitoring.

Most of the capabilities mentioned below are universal for all types of volcanic systems, although some are best applied to stratovolcanoes with an apical single vent. In some settings, such as calderas or shield volcanoes, we must broaden coverage to include multiple possible storage regions or vent locations. As an example, Thelen (2014) discretized the long rift zones of shield volcanoes in Hawaiʻi as a set of evenly spaced "vents." In this construct, each vent comes with recommendations, and several thousand network configurations were simulated to assess the effect on network quality levels and to determine the most efficient network design. The same process could be applied in a caldera setting or a volcanic field, where an evenly spaced grid of potential vents is considered. Localized recommendations for each unique system are beyond the scope of this report and left up to local experts to assess based on the conditions, restrictions, and requirements of each volcano.

Recommended Capabilities

Detect Changes in Earthquake Location, Seismic Energy Release, Event Type, and Source Properties

Marked increases in earthquake rates have been observed at erupting volcanoes as diverse in size, chemistry, and eruptive style as Kīlauea, Hawaiʻi (Klein and others, 1987); Mount St. Helens, Washington (Malone and others, 1981; Moran and others, 2008a); and Mount Pinatubo, Philippines (Harlow and others, 1996). Depending on the volcano, precursory seismic sequences may be entirely composed of smaller magnitude ($M<2$) earthquakes; for example, at Mount Spurr, Alaska, in 1992 (Power and others, 1995). Earthquake hypocenters have also been observed to migrate in advance of eruptions (for example, Klein and others, 1987; Harlow and others, 1996; Battaglia and others, 2005; Nakada and others, 2005). Finally, relocation of similar events ("multiplets") has yielded precise relative locations, particularly when paired with matched filter techniques, which have proven useful for constraining magmatic processes in conduits (for example, Prejean and others, 2003; Shelly and others, 2013; Shelly and Thelen, 2019). Machine learning (ML) approaches are improving detection and location capabilities (for example, Wilding and others, 2022). Generally, the infrastructure requirements for ML approaches overlap entirely with the capabilities above. Most of the examples above are specific to volcano-tectonic earthquakes, and the ability to identify these types of events and assess changes in space and time are a critical capability for any volcano observatory.

In addition to volcano-tectonic earthquakes, volcanism is commonly associated with other types of seismicity, including seismic tremor, very long period (VLP) earthquakes, hybrid earthquakes, and low-frequency earthquakes. In a variety of unrest and eruption scenarios these non-standard types of earthquakes may dominate over volcano-tectonic seismicity, underscoring their importance in monitoring. Changes in seismicity have been observed before many eruptions, such as from dominantly volcano-tectonic to dominantly low-frequency

earthquakes in the hours, days, and weeks preceding the onset of eruptive activity at Mount St. Helens in 1980–86 and 2004 (Endo and others, 1981; Malone and others, 1983; Moran and others, 2008b), Mount Pinatubo in 1991 (Harlow and others, 1996), and Soufrière Hills in 1995 (Gardner and White, 2002). Automated techniques to differentiate between event types are especially important during unrest when high earthquake rates may overwhelm analysts. Some automated machine learning approaches are becoming more widely applied (for example, Bueno and others, 2020; Tan and others, 2023). It is also important to be able to characterize deep activity, such as deep long-period earthquakes, that may be precursors to eruptions (for example, White, 1996; Power and others, 2013; Frank and others, 2018).

Seismic tremor is commonly recognized during unrest and eruption. However, real-time analysis is typically limited to time series of amplitude and frequency content. In some eruptions, such as Pavlof Volcano in 2016 (Fee and others, 2017), seismicity was dominated by seismic tremor, with only a few discrete earthquakes identified and no precursory seismicity. Detection and tracking of seismic tremor have proven important at several volcanoes for accurate eruption forecasting and tracking of ongoing eruptions (for example, McNutt and others, 1995; Takagi and others, 2006; Hotovec and others, 2013). Locating seismic tremor using amplitude-based techniques (for example, Battaglia and Aki, 2003; Taisne and others, 2011) or network covariance (for example, Soubestre and others, 2019; Maher and others, 2023) is feasible in real time and important for monitoring dike intrusions and eruptions.

An additional recommended capability for seismic monitoring is on-scale recording of seismicity without clipping. Clipping of a seismic trace can occur during strong ground motion when the recording capabilities of the seismometer or digitizer are exceeded. Tracking long-term seismicity rates and energy release through techniques such as real-time seismic-amplitude measurement (Endo and Murray, 1991) at volcanoes has repeatedly proven to be an effective means of recognizing renewed volcanic activity. At some energetic volcanoes, however, seismicity before and (or) accompanying an eruption intensifies to the point where low-dynamic-range seismic systems within a few kilometers become saturated and cannot be used for tracking changes in seismicity and earthquake magnitudes (Endo and others, 1981; Malone and others, 1981; Moran and others, 2008b). This problem can be mostly solved by installing modern digitizers (24+ bit), thus greatly increasing the seismic-energy range over which on-scale recording can be obtained and ensuring the ability to track changes in seismic-energy release, event rate, and event type during the most energetic phases of a precursory or eruptive sequence. In cases where strong seismicity (>*M*4) has been observed or is expected, the dynamic range of a 24-bit digitizer-broadband combination may be exceeded within a few kilometers of the seismic source, and a strong-motion instrument co-located with a broadband seismometer within 10 kilometers (km) of an eruption site would ensure on-scale recording despite strong earthquakes and (or) tremor.

Instrumentation

In principle, a single seismic station can be used to track earthquake rate and record qualitative changes in seismic-energy release; however, at least two stations are required for robustly distinguishing between the signals produced by volcanic and nonvolcanic (for example, wind, anthropogenic noise, electronic interference) phenomena. For all location methods described above, at least four seismic observations are required to locate earthquakes and constrain the timing, but to optimize location quality, it is best to have eight or more observations. Fewer observations may be acceptable based on station distribution. Ideally, these sites would be clustered around areas of high seismicity to constrain the smallest events. But for deep long-period earthquakes, or earthquakes associated with offset magma transport systems, having a larger spread in stations is optimal, meaning more than eight sites are likely required for most systems. To track changes in depth, it is critical to have at least one station above the seismic source, which commonly means as close to the expected vent of the volcano as feasible (fig. B1). In many cases,

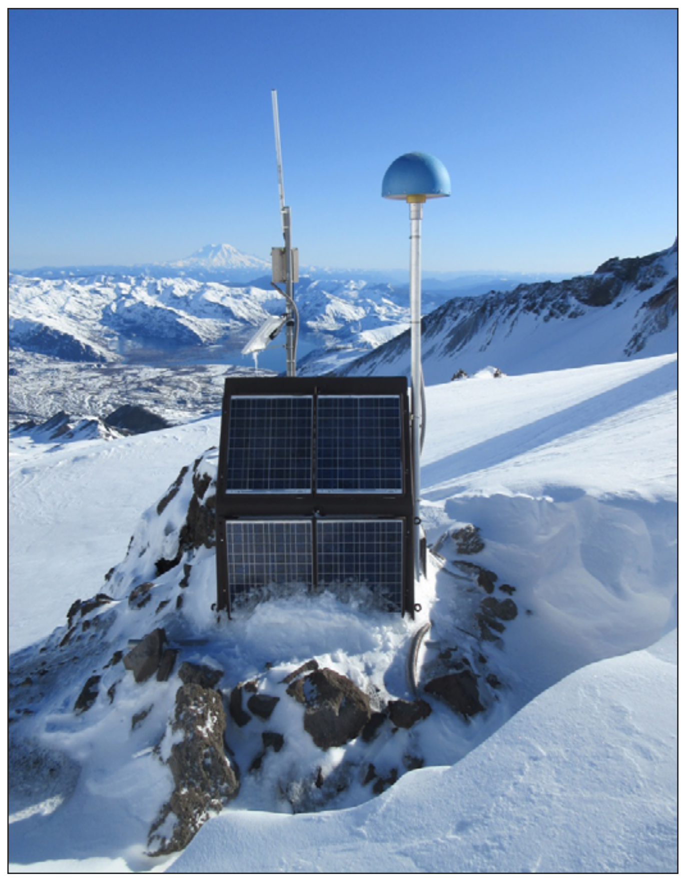

Figure B1. Photograph of monitoring station September Lobe (SEP) on the 1980–86 dome at Mount St. Helens, Washington. The site has co-located seismic, geodetic, tilt, and infrasound instruments. View is to the north; Spirit Lake is visible in the near-background and Mount Rainier is on the skyline. Photograph by Ben Pauk, U.S. Geological Survey, 2018.

logistical constraints such as glacier coverage, winter snow and ice conditions, volcanic hazard, telemetry, or land-use restrictions may preclude the installation of a station directly above the source of the earthquakes. In these cases, a small-aperture seismic array at the nearest practical site may offer the ability to track changes in depth very precisely through the calculation of an incidence angle (for example, Glasgow and others, 2018). Short-period, vertical-component instruments may be sufficient for some of the capabilities mentioned above; however, earthquake-location accuracy, especially in depth, is improved when S-wave arrival times are included, which are more reliably identified by using three-component seismometers. Moreover, adequate detection of all types of volcanic seismicity requires broadband sensitivity (120 seconds to 50 hertz). In the past decade, broadband seismometers have become more cost effective and require dramatically less power; thus, these instruments have become the preferred type of seismometer for volcano monitoring. If moderate earthquakes (>*M*4) or large explosions are expected at a given volcano, then at least one strong-motion sensor would ideally be co-located with a broadband seismometer within 10 km of an expected vent to provide on-scale recordings during unrest.

Recommendations

For level 1 volcanoes, the ideal network would be able to detect >*M*1.5 earthquakes and to locate (crudely) >*M*3 earthquakes. For level 2 volcanoes, the network would detect >*M*1 earthquakes, crudely locate >*M*2 earthquakes, and detect energetic seismic tremor. For level 3 volcanoes, the network would detect >*M*0.5 earthquakes and to accurately locate >*M*1 earthquakes while recording and distinguishing between all event types and detecting seismic tremor. For level 4 volcanoes, the network would detect and accurately locate >*M*0 earthquakes, determine event type, detect and locate seismic tremor, and provide on-scale recordings of energetic seismicity.

Detect Changes in Localized Stress Fields

Understanding the stress state within a volcano and how those stresses change over time is a key contribution of seismology to assessing volcanic hazards. Magma intrusions have been correlated with changes to the local stress field that overprint the background stress-field orientations. As such, they can provide some of the earliest clues of unrest related to magma intrusion, even during times when seismicity rates are near background. Stress-field changes have been detected during periods of quiescence, unrest, and eruption by (1) changes in fault-plane solutions (for example, Moran, 1994; Roman and others, 2004; Sánchez and others, 2004), (2) changes in *b*-value (the slope of the frequency-magnitude distribution) (Vinciguerra, 2002; Novelo-Casanova and others, 2006), and (3) changes in shear-wave-splitting directions (for example, Miller and Savage, 2001; Gerst and Savage, 2004; Johnson and Poland, 2013).

Stress rotations have been observed through analysis of fault-plane solutions in preeruptive sequences worldwide (Roman and Cashman, 2006). These stress rotations commonly differ from a background or regional direction prior to eruption and may be used to assess the likelihood of eruption (Roman and others, 2006). Further scrutiny of fault-plane solutions in space and time led to an estimation of viscosity during the 2018 eruption at Kīlauea (Roman and others, 2021). Automated fault-plane solutions can be calculated in near-real time (<5 minutes) if events are constrained by sufficient observations (see below).

Within an earthquake catalog, the rate of decrease of earthquake frequency with increasing size can be quantified by a *b*-value, which provides insight into the integration of cracks into longer fractures and faults that can fail as larger earthquakes. Vinciguerra (2002) used earthquake-catalog data to investigate temporal changes in *b*-values before and during the 1989 eruption of Mount Etna and reported precursory changes. Monitoring of temporal *b*-value changes requires real-time earthquake detection. Monitoring of spatial *b*-value changes requires real-time earthquake location, and thus multiple stations, and is difficult during vigorous seismic swarms.

When S-waves from regional earthquakes encounter anisotropy in the crust, they split into two new orthogonal waves that can be used to map out subsurface features (for example, underneath volcanoes). Changes in S-wave-splitting directions were reported by Miller and Savage (2001) and Gerst and Savage (2004) in association with the 1998 eruption of Mount Ruapehu; these authors inferred that the changes in S-wave-splitting direction were caused by intrusion of a 10-km-long dike. As with fault-plane solutions, S-wave-splitting directions can be calculated relatively rapidly if there are sufficient observations on a three-component network of seismometers.

Instrumentation

Fault-plane solutions, especially for volcano-tectonic earthquakes, are most commonly calculated from first-motion data. Source mechanisms also can be determined from P- to S- amplitude ratios (Julian and others, 1998; Pugh and others, 2016) or waveform modeling at long periods (for example, Chouet and others, 2003). Fault-plane solutions generally are poorly determined with fewer than 7 first motions and are most reliable with 10 or more first motions that are well distributed in azimuth and distance around the earthquake epicenter. Source mechanisms considering non-double couple sources, common in volcanic regions, require more data to constrain more unknowns. Amplitude ratios between P- and S-waves can also be used (Julian and others, 1998; Snoke, 2003; Pugh and others, 2016), but reliable S-wave picks require three-component sensors. Quality fault-plane solutions are also dependent on a quality velocity model and many non-double couple sources can be attributed to a poor velocity model or too few observations. To distinguish between temporal and spatial *b*-value changes, a seismic network must be able to locate events to within 1-km accuracy. Because *b*-values are more accurately determined over a wide range of

event magnitudes, on-scale recordings of earthquakes are essential for a quality magnitude calculation. S-wave splitting has been detected exclusively on broadband seismometers, although in principle S-wave splitting could be done with short-period, three-component sensors. Instruments must be deployed directly above the volume of interest. In addition, for a rapid S-wave splitting determination, S-waves must be timed on both horizontal channels, which is not commonplace for networks within the United States. S-wave picks can also be made using machine learning (for example, Zhu and Beroza, 2019).

Recommendations

For levels 1 and 2 volcanoes, this capability is not required. For level 3 volcanoes, it is advisable to quantify generalized stress fields near the volcanic center using fault-plane solutions and *b*-values for earthquakes >*M*1. For level 4 volcanoes, one can detect detailed stress-field changes, such as stress rotations, by constructing well-constrained fault-plane solutions and (or) moment tensors, non-double couple fault-plane solutions, mapping *b*-values at high spatial resolution, and detecting changes in S-wave-splitting directions over time.

Monitor Changes in Seismic Source and (or) Path Over Time

As magma intrudes into or beneath a volcanic edifice, it can compress pore spaces, open or close cracks, and otherwise affect the country rock surrounding the conduit. These changes will likely change the local bulk-rock properties (density, compressibility, and yield strength) of the subsurface and may produce observable changes in seismic velocity, attenuation, or source mechanism over time. Detection of these material changes in the subsurface can be important to understanding the causes of magma unrest and the potential for eruption.

Temporal changes in seismic velocity have been observed at several volcanic centers, most recently using ambient noise techniques (for example, Brenguier and others, 2008). At Piton de la Fournaise, decreases in seismic velocity occurred prior to several eruptions (Brenguier and others, 2008). At Kīlauea, changes in velocity were strongly correlated to changes in tilt, an exciting development at volcanoes without tiltmeters installed (Donaldson and others, 2017). Although the studies mentioned above use pairs of stations, Bennington and others (2018) used a single station at Mount Veniaminof, Alaska, to find precursory eruptive velocity changes and localize the depth of the velocity change.

Spatial and temporal changes in seismic velocity, sometimes referred to as four-dimensional tomography, could influence the assessment of volcanic hazard by combining emerging techniques. Knowing where magma is stored and transported assists in developing a conceptual model for understanding unrest. The utility of repeat travel time tomography has been demonstrated in some settings, where changes in the V_P/V_S ratio can be observed (Koulakov and others, 2013; Koulakov and Vargas, 2018). Using catalogs improved through matched filtering or machine learning approaches may allow for more frequent and higher resolution tomography. Additionally, the length of continuous data records critical for ambient noise tomography is growing, allowing for repeated studies where an ambient noise model has already been calculated (for example, Brenguier and others, 2007; Flinders and Shen, 2017; Flinders and others, 2018).

Changes in country rock, such as fracturing or fluid injection, can also affect scattering properties of the medium, which influence the codas (tails) of individual earthquake seismograms. Recently, researchers have compared repeating earthquakes to show that variations occur only in the coda, a phenomenon that can be caused only by changes in country rock between the earthquake and the seismometer. Velocity changes were found in association with activity at Mount St. Helens (Hotovec-Ellis and others, 2014, 2015) and Kīlauea (Hotovec-Ellis and others, 2022).

Finally, changes in the properties of long-period events have been used to infer changes in magmatic systems over time. At Galeras volcano, Colombia, Gómez and Torres (1997) reported that coda durations increased and dominant frequencies decreased in long-period “tornillo”-type events before dome-damaging explosions. Kumagai and others (2001) showed that the characteristics of long-period seismic signals can change based on the proportion of gas, magma, and ash inside the resonating crack.

Instrumentation and Recommendations

For level 1 volcanoes, this capability is not required. For level 2 volcanoes, long-period events would ideally be detectable, as should event families for >*M*1 earthquakes. The network would be capable of detecting broad-scale changes in velocity over long periods of time. At level 3 volcanoes, the network would be able to detect long-period earthquakes and event families for >*M*0.5 earthquakes and to detect changes in travel time and broad-scale changes in seismic velocity over long periods of time. For level 4 volcanoes, the network would allow for determination of temporal source properties of long-period earthquakes, detection and location of event families for >*M*0 events, and construction of time-varying three-dimensional velocity models (provided local seismicity or seismic noise is sufficient).

Detect and Determine Source Mechanisms for Very Long Period and Long Period Events

As seismic networks have become denser and more sensitive to low frequencies, scientists have increasingly detected the occurrence of very long period (VLP) waves that may reflect the shallow movement of large volumes of magma or volcanic fluids related to intrusion and volcanic unrest. These VLP events manifest in discrete events (for example, Arciniega-Ceballos and others, 1999; Hidayat and others, 2000; Kumagai and others, 2001) and tremor (for example, De Lauro and others, 2005; Haney, 2010). VLP events or VLP tremor can be located using particle motions in a technique called radial semblance (Almendros and Chouet, 2003; Dawson and others, 2004). With the proper number and distribution

of broadband instrumentation, one can determine through the moment tensor the orientation and dimensions of the crack or sill that is generating the VLP and (or) long-period energy, providing critical information on the geometry of shallow parts of the magma plumbing system (Chouet and Dawson, 2011). Obtaining the moment tensor that helps define the plumbing system geometry is difficult in real time because of the complexity of volcanic topography and structure. In addition, calculating the moment tensor with waveform modeling is computationally intensive but potentially tractable in the near future (Auger and others, 2006). However, for multiyear eruptions or repeated eruptions that reuse shallow parts of the magma plumbing system, even results calculated weeks after an event can be useful for monitoring.

Instrumentation

VLP events can be detected with just two broadband sensors, although the sensors should be placed within a few wavelengths of the source epicenter (<5 km typically). Locating these events requires at least three broadband stations (preferably more to reduce errors) located within 5 km of the source epicenter (Dawson and others, 2004). At least three broadband stations within 5 km of the vent are required to completely determine all elements of the moment-tensor matrix as well as the location and single force terms, but typically such calculations are done with more than 10 stations. Such a high number of stations so close to an eruptive vent is only possible at a few volcanoes or for a limited temporary deployment. Where the geography allows and VLP activity has been documented, a dense network of broadband stations within 5 km would ideally be the goal. VLP earthquakes correlated with caldera collapse (Kumagai and others, 2001; Fontaine and others, 2019; Flinders and others, 2020) and large step-like inflations and (or) deflations can be substantially biased by band-limited seismometer response and are best interpreted with near station or co-located Global Navigation Satellite System (GNSS) data (Flinders and others, 2021).

Recommendations

For levels 1 and 2 volcanoes, this capability is not required. For level 3 volcanoes, the network would be able to detect VLP signals. For level 4 volcanoes, the network would detect and locate VLP events and track relative movement of the VLP source if the geography and land-use restrictions are permissive.

General Recommendations and Considerations

Broadband seismometers would ideally be prioritized over short-period seismometers because of the added sensitivity at low frequencies and added capabilities for volcano research purposes (for example, receiver functions and moment tensor inversions). There are several volcanic processes (described above) that generate low frequency seismic signals that benefit from observations only made possible through broadband instrumentation. With the added sensitivity comes added requirements for vaults that minimize thermal fluctuations and electronic noise. There have been substantial advances in vault testing and design with Transportable Array and ShakeAlert system buildouts, and future installations would follow as many of those design criteria as is feasible given the accessibility of the site and land-use restrictions (fig. B2). Broadband instruments also have a demonstrated sensitivity to tilt that could be useful during unrest if the sensor is sufficiently close to the source and inside a thermally stable vault (Lyons and others, 2012). The minimum sample rate for new installations is 50 samples per second, but 100 samples per second would be an ideal goal. This higher sample rate allows for more precise determination of P- and S-wave arrivals, higher precision lag estimates (good for relocations), earthquake waveform modeling, and more accurate polarities for focal mechanisms. Continuous low-latency seismic data are required, and efforts would ideally be made to comply with the U.S. Geological Survey’s Earthquake Hazards Program Advanced National Seismic System (ANSS) performance standards where and when appropriate (U.S. Geological Survey, 2017; U.S. Geological Survey Earthquake Hazards Program, 2019).

Figure B2. Photograph of a U.S. Geological Survey field technician performing site maintenance on seismic station ISLZ on Unimak Island, central Aleutian Islands, Alaska. Photograph by Dane Ketner, U.S. Geological Survey, August 15, 2020.

Summary—Recommendations for Volcano Levels 1–4 Seismic Networks

Level 1.—Five seismic stations within 200 km of the volcanic center, including two stations within 50 km.

Level 2.—Five seismic stations within 50 km of the volcanic center, including two stations within 10 km.

Level 3.—Seven or more broadband seismic stations within 20 km of the volcanic center, including at least two stations within 5 km.

Level 4.—Twelve to 25 broadband seismic stations within 20 km of the volcanic center, including at least 8 stations within 10 km and 4 or more within 5 km; at least one broadband or strong-motion station within 10 km. Small-aperture seismic array in places where logistics preclude placing stations high on the edifice.

References Cited

Almendros, J., and Chouet, B., 2003, Performance of the radial semblance method for the location of very long period volcanic signals: Bulletin of the Seismological Society of America, v. 93, no. 5, p. 1890–1903, https://doi.org/10.1785/0120020143.

Arciniega-Ceballos, A., Chouet, B.A., and Dawson, P.B., 1999, Very long-period signals associated with Vulcanian explosions at Popocatepetl Volcano, Mexico: Geophysical Research Letters, v. 26, no. 19, p. 3013–3016, https://doi.org/10.1029/1999GL005390.

Auger, E., D'Auria, L., Martini, M., Chouet, B., and Dawson, P., 2006, Real-time monitoring and massive inversion of source parameters of very long period seismic signals—An application to Stromboli Volcano, Italy: Geophysical Research Letters, Solid Earth, v. 33, no. 4, 5 p., https://doi.org/10.1029/2005GL024703.

Battaglia, J., and Aki, K., 2003, Location of seismic events and eruptive fissures on the Piton de la Fournaise volcano using seismic amplitudes: Journal of Geophysical Research Solid Earth, v. 108, no. B8, article no. 2364.

Battaglia, J., Ferrazzini, V., Staudacher, T., Aki, K., and Cheminée, J.L., 2005, Pre-eruptive migration of earthquakes at the Piton de la Fournaise volcano (Réunion Island): Geophysical Journal International, v. 161, no. 2, p. 549–558, https://doi.org/10.1111/j.1365-246X.2005.02606.x.

Bennington, N., Haney, M., Thurber, C., and Zeng, X., 2018, Inferring magma dynamics at Veniaminof volcano via application of ambient noise: Geophysical Research Letters, v. 45, no. 21, p. 11,650–11,658, https://doi.org/10.1029/2018GL079909.

Brenguier, F., Shapiro, N.M., Campillo, M., Ferrazzini, V., Duputel, Z., Coutant, O., and Nercessian, A., 2008, Towards forecasting volcanic eruptions using seismic noise: Nature Geoscience, v. 1, no. 2, p. 126–130, https;//doi.org/10.1038/ngeo104.

Brenguier, F., Shapiro, N.M., Campillo, M., Nercessian, A., and Ferrazzini, V., 2007, 3-D surface wave tomography of the Piton de la Fournaise Volcano using seismic noise correlations: Geophysical Research Letters, Solid Earth, v. 34, no. 2, https://doi.org/10.1029/2006GL028586.

Bueno, A., Zuccarello, L., Díaz-Moreno, A., Woollam, J., Titos, M., Benítez, C., Álvarez, I., Prudencio, J., and de Angelis, S., 2020, PICOSS—Python interface for the classification of seismic signals: Computers and Geosciences, v. 142, no. 104531, https://doi.org/10.1016/j.cageo.2020.104531.

Chouet, B., and Dawson, P., 2011, Shallow conduit system at Kilauea Volcano, Hawaii, revealed by seismic signals associated with degassing bursts: Journal of Geophysical Research, Solid Earth, v. 116, no. B12, https://doi.org/10.1029/2011JB008677.

Chouet, B., Dawson, P., Ohminato, T., Martini, M., Saccorotti, G., Giudicepietro, F., De Luca, G., Milana, G., and Scarpa, R., 2003, Source mechanisms of explosions at Stromboli Volcano, Italy, determined from moment-tensor inversions of very-long-period data: Journal of Geophysical Research, Solid Earth, v. 108, no. B1, p. ESE 7-1–ESE 7-25, https://doi.org/10.1029/2002JB001919.

Dawson, P., Whildin, D., and Chouet, B., 2004, Application of near real-time radial semblance to locate the shallow magmatic conduit at Kīlauea Volcano, Hawaii: Geophysical Research Letters, Solid Earth, v. 31, no. 21, 4 p., https://doi.org/10.1029/2004GL021163.

De Lauro, E., De Martino, S., Falanga, M., Palo, M., and Scarpa, R., 2005, Evidence of VLP volcanic tremor in the band [0.2–0.5] Hz at Stromboli Volcano, Italy: Geophysical Research Letters, Solid Earth, v. 32, no. 17, 4 p., https://doi.org/10.1029/2005GL023466.

Donaldson, C., Caudron, C., Green, R.G., Thelen, W.A., and White, R.S., 2017, Relative seismic velocity variations correlate with deformation at Kīlauea volcano: Science Advances, v. 3, no. 6, https://doi.org/10.1126/sciadv.1700219.

Endo, E.T., Malone, S.D., Noson, L.L., and Weaver, C.S., 1981, Locations, magnitudes, and statistics of the March 20–May 18 earthquake sequence, *in* Lipman, P.W., and Mullineaux, D.R., eds., The 1980 eruptions of Mount St. Helens: U.S. Geological Survey Professional Paper 1250, p. 93–107, https://doi.org/10.3133/pp1250.

Endo, E.T., and Murray, T., 1991, Real-time seismic amplitude measurement (RSAM); a volcano monitoring and prediction tool: Bulletin of Volcanology, v. 53, p. 533–545, https://doi.org/10.1007/BF00298154.

Fee, D., Haney, M.M., Matoza, R.S., Van Eaton, A.R., Cervelli, P., Schneider, D.J., and Iezzi, A.M., 2017, Volcanic tremor and plume height hysteresis from Pavlof Volcano, Alaska: Science v. 355, p. 45–48, https://doi.org/10.1126/science.aah6108.

Flinders, A.F., Johanson, I.A., Dawson, P.B., Anderson, K.R., Haney, M.M., and Shiro, B.R., 2020, Very-long-period (VLP) seismic artifacts during the 2018 caldera collapse at Kīlauea, Hawaiʻi: Seismological Research Letters, v. 91, no. 6, p. 3417–3432, https://doi.org/10.1785/0220200083.

Flinders, A.F., Kauahikaua, J.P., Hsieh, P.A., and Ingebritsen, S.E., 2021, Post audit of simulated groundwater flow to the short-lived (2019 to 2020) crater lake at Kīlauea volcano, Hawaiʻi: Groundwater, v. 60, no. 1, p. 2–155, https://doi.org/10.1111/gwat.13133.

Flinders, A.F., Shelly, D.R., Dawson, P.B., Hill, D.P., Tripoli, B., and Shen, Y., 2018, Seismic evidence for significant melt beneath the Long Valley Caldera, California, USA: Geology, v. 46, p. 799–802, https://doi.org/10.1130/G45094.1.

Flinders, A.F., and Shen, Y., 2017, Seismic evidence for a possible deep crustal hot zone beneath southwest Washington: Scientific Reports, v. 7, article no. 7400, https://doi.org/10.1038/s41598-017-07123-w.

Fontaine, F.R., Roult, G., Hejrani, B., Michon, L., Ferrazzini, V., Barruol, G., Tkalčić, H., Di Muro, A., Peltier, A., Reymond, D., Staudacher, T., and Massin, F., 2019, Very- and ultra-long-period seismic signals prior to and during caldera formation on La Réunion Island: Scientific Reports, v. 9, article no. 8068, https://doi.org/10.1038/s41598-019-44439-1.

Frank, W.B., Shapiro, N.M., and Gusev, A.A., 2018, Progressive reactivation of the volcanic plumbing system beneath Tolbachik Volcano (Kamchatka, Russia) revealed by long-period seismicity: Earth and Planetary Science Letters, v. 493, p. 47–56, https://doi.org/10.1016/j.epsl.2018.04.018.

Gardner, C.A., and White, R.A., 2002, Seismicity, gas emission and deformation from 18 July to 25 September 1995 during the initial phreatic phase of the eruption of Soufrière Hills Volcano, Montserrat, *in* Druitt, T.H., and Kokelaar, B.P., eds., The eruption of Soufrière Hills Volcano, Montserrat, from 1995 to 1999: Geological Society of London Memoirs, v. 21, p. 567–581, https://doi.org/10.1144/GSL.MEM.2002.021.01.26.

Gerst, A., and Savage, M.K., 2004, Seismic anisotropy beneath Ruapehu Volcano—A possible eruption forecasting tool: Science, v. 306, no. 5701, p. 1543–1547, https://doi.org/10.1126/science.1103445.

Glasgow, M.E., Schmandt, B., and Hansen, S.M., 2018, Upper crustal low-frequency seismicity at Mount St. Helens detected with a dense geophone array: Journal of Volcanology and Geothermal Research, v. 358, p. 329–341, https://doi.org/10.1016/j.jvolgeores.2018.06.006.

Gómez, D.M., and Torres C., R.A., 1997, Unusual low-frequency volcanic seismic events with slowly decaying coda waves observed at Galeras and other volcanoes: Journal of Volcanology and Geothermal Research, v. 77, no. 1–4, p. 173–193, https://doi.org/10.1016/S0377-0273(96)00093-5.

Haney, M.M., 2010, Location and mechanism of very long period tremor during the 2008 eruption of Okmok Volcano from interstation arrival times: Journal of Geophysical Research, v. 115, no. B10, https://doi.org/10.1029/2010JB007440.

Harlow, D.H., Power, J.A., Laguerta, E.P., Ambubuyog, G., White, R.A., and Hoblitt, R.H., 1996, Precursory seismicity and forecasting of the June 15, 1991, eruption of Mount Pinatubo, *in* Newhall, C.S., and Punongbayan, S., Fire and mud—Eruptions and lahars of Mount Pinatubo, Philippines: Seattle, University of Washington Press, p. 285–305.

Hidayat, D., Voight, B., Langston, C., Ratdomopurbo, A., and Ebeling, C., 2000, Broadband seismic experiment at Merapi Volcano, Java, Indonesia—Very-long-period pulses embedded in multiphase earthquakes: Journal of Volcanology and Geothermal Research, v. 100, no 1–4, p. 215–231, https://doi.org/10.1016/S0377-0273(00)00138-4.

Hotovec, A.J., Prejean, S.G., Vidale, J.E., and Gomberg, J., 2013, Strongly gliding harmonic tremor during the 2009 eruption of Redoubt Volcano: Journal of Volcanology and Geothermal Research, v. 259, p. 89–99, https://doi.org/10.1016/j.jvolgeores.2012.01.001.

Hotovec-Ellis, A.J., Gomberg, J., Vidale, J.E., and Creager, K.C., 2014, A continuous record of intereruption velocity change at Mount St. Helens from coda wave interferometry: Journal of Geophysical Research, Solid Earth, v. 119, no. 3, p. 2199–2214, https://doi.org/10.1002/2013JB010742.

Hotovec-Ellis, A.J., Shiro, B.R., Shelly, D.R., Anderson, K.R., Haney, M.M., Thelen, W.A., Montgomery-Brown, E.K., and Johanson, I.A., 2022, Earthquake-derived seismic velocity changes during the 2018 caldera collapse of Kīlauea volcano: Journal of Geophysical Research Solid Earth, v. 127, no. 2, https://doi.org/10.1029/2021JB023324.

Hotovec-Ellis, A.J., Vidale, J.E., Gomberg, J., Thelen, W., and Moran, S.C., 2015, Changes in seismic velocity during the first 14 months of the 2004–2008 eruption of Mount St. Helens, Washington: Journal of Geophysical Research, Solid Earth, v. 120, no. 9, p. 6226–6240, https://doi.org/10.1002/2015JB012101.

Johnson, J.H., and Poland, M.P., 2013, Seismic detection of increased degassing before Kīlauea's 2008 summit explosion: Nature Communications, v. 4, no. 1668, https://doi.org/10.1038/ncomms2703.

Julian, B., Miller, A.D., and Foulger, G.R., 1998, Non-double-couple earthquakes—1. Theory: Reviews of Geophysics, v. 36, no. 4, p. 525–549, https://doi.org/10.1029/98RG00716.

Klein, F.W., Koyanagi, Y., Nakata, J.S., and Tanigawa, W.R., 1987, The seismicity of Kīlauea's magma system, *in* Decker, R.W., Wright, T.L., Stauffer, P.H., eds., Volcanism in Hawaii: U.S. Geological Survey Professional Paper 1350, p. 1019–1185, https://doi.org/10.3133/pp1350.

Koulakov, I., and Vargas, C.A., 2018, Evolution of the magma conduit beneath the Galeras Volcano inferred from repeated seismic tomography: Geophysical Research Letters, v. 45, no. 15, p. 7514–7522, https://doi.org/10.1029/2018GL078850.

Koulakov, I., West, M., and Izbekov, P., 2013, Fluid ascent during the 2004–2005 unrest at Mt. Spurr inferred from seismic tomography: Geophysical Research Letters, v. 40, no. 17, p. 4579–4582, https://doi.org/10.1002/grl.50674.

Kumagai, H., Ohminato, T., Nakano, M., Ooi, M., Kubo, A., Inoue, H., and Oikawa, J., 2001, Very-long-period seismic signals and caldera formation at Miyake Island, Japan: Science, v. 293, no. 5530, p. 687–690, https://doi.org/10.1126/science.1062136.

Lyons, J.J., Waite, G.P., Ichihara, M., and Lees, J.M., 2012, Tilt prior to explosions and the effect of topography on ultra-long-period seismic records at Fuego volcano, Guatemala: Geophysical Research Letters, v. 39, no. 8, p. L08305.

Maher, S.P., Dawson, P., Hotovec-Ellis, A., Thelen, W.A., Jolly, A., Bennington, N., Chang, J.C., and Dotray, P., 2023, Characterizing and locating seismic tremor during the 2022 eruption of Mauna Loa volcano, Hawaiʻi, with network covariance: The Seismic Record, v. 3, no. 3, p. 228–238, https://doi.org/10.1785/0320230020.

Malone, S.D., Boyko, C., and Weaver, C.S., 1983, Seismic precursors to the Mount St. Helens eruptions in 1981 and 1982: Science, v. 221, no. 4618, p. 1376–1378, https://doi.org/10.1126/science.221.4618.1376.

Malone, S.D., Endo, E.T., Weaver, C.S., and Ramey, J.W., 1981, Seismic monitoring for eruption prediction, *in* Lipman, P.W., and Mullineaux, D.R., eds., The 1980 eruptions of Mount St. Helens: U.S. Geological Survey Professional Paper 1250, p. 803–813, https://doi.org/10.3133/pp1250.

McNutt, S.R., Tytgat, G.C., and Power, J.A., 1995, Preliminary analyses of volcanic tremor associated with 1992 eruptions of Crater Peak, Mount Spurr Volcano, Alaska, *in* Keith, T.E.C., ed., The 1992 eruptions of Crater Peak vent, Mount Spurr Volcano, Alaska: U.S. Geological Survey Bulletin 2139, p. 161–178, https://doi.org/10.3133/b2139.

Miller, V., and Savage, M., 2001, Changes in seismic anisotropy after volcanic eruptions—Evidence from Mount Ruapehu: Science, v. 293, no. 5538, p. 2231–2233, https://doi.org/10.1126/science.1063463.

Moran, S.C., 1994, Seismicity at Mount St. Helens, 1987–1992—Evidence for repressurization of an active magmatic system: Journal of Geophysical Research, Solid Earth, v. 99, no. B3, p. 4341–4354, https://doi.org/10.1029/93JB02993.

Moran, S.C., Malone, S.D., Qamar, A.I., Thelen, W.A., Wright, A.K., and Caplan-Auerbach, J., 2008a, Seismicity associated with renewed dome-building at Mount St. Helens, 2004–2005, *in* Sherrod, D.R., Scott, W.E., and Stauffer, P.H., eds., A volcano rekindled—The renewed eruption of Mount St. Helens, 2004–2006: U.S. Geological Survey Professional Paper 1750, p. 27–60, https://doi.org/10.3133/pp1750.

Moran, S.C., McChesney, P.J., and Lockhart, A.B., 2008b, Seismicity and infrasound associated with explosions at Mount Saint Helens, 2004–2005, *in* Sherrod, D.R., Scott, W.E., and Stauffer, P.H., eds., A volcano rekindled—The renewed eruption of Mount St. Helens, 2004–2006: U.S. Geological Survey Professional Paper 1750, p. 111–127, https://doi.org/10.3133/pp1750.

Nakada, S., Uto, K., Sakuma, S., Eichelberger, J.C., and Shimizu, H., 2005, Scientific results of conduit drilling in the Unzen Scientific Drilling Project (USDP): Scientific Drilling, v. 1, p. 18–22, https://doi.org/10.2204/iodp.sd.3.01.2006.

Novelo-Casanova, D.A., Martínez-Bringas, A., and Valdés-González, C., 2006, Temporal variations of Q_c^{-1} and *b*-values associated to the December 2000–January 2001 volcanic activity at the Popocatepetl Volcano, Mexico: Journal of Volcanology and Geothermal Research, v. 152, no. 3–4, p. 347–358, https://doi.org/10.1016/j.jvolgeores.2005.10.003.

Power, J.A., Jolly, A.D., Page, R.A., and McNutt, S.R., 1995, Seismicity and forecasting of the 1992 Eruptions of Crater Peak vent, Mount Spurr Volcano, Alaska—An overview, *in* The 1992 Eruptions of Crater Peak vent, Mount Spurr Volcano, Alaska: U.S. Geological Survey Bulletin 2139, p. 149–159, http://doi.org/10.3133/b2139.

Power, J.A., Stihler, S.D., Chouet, B.A., Haney, M.M., and Ketner, D.M., 2013, Seismic observations of redoubt volcano, Alaska—1989–2010 and a conceptual model of the redoubt magmatic system: Journal of Volcanology and Geothermal Research, v. 259, p. 31–44.

Prejean, S., Stork, A., Ellsworth, W., Hill, D., and Julian, B., 2003, High precision earthquake locations reveal seismogenic structure beneath Mammoth Mountain, California: Geophysical Research Letters, Solid Earth, v. 30, no. 24, https://doi.org/10.1029/2003GL018334.

Pugh, D.J., White, R.S., and Christie, P.A.F., 2016, A Bayesian method for microseismic source inversion: Geophysical Journal International, v. 206, no. 2, p. 1009–1038, https://doi.org/10.1093/gji/ggw186.

Roman, D.C., and Cashman, K.V., 2006, The origin of volcano-tectonic earthquake swarms: Geology, v. 34, no. 6, p. 457–460, https://doi.org/10.1130/G22269.1.

Roman, D.C., Moran, S.C., Power, J.A., and Cashman, K.V., 2004, Temporal and spatial variation of local stress fields before and after the 1992 eruptions of Crater Peak vent, Mount Spurr volcano, Alaska: Bulletin of the Seismological Society of America, v. 94, no. 6, p. 2366–2379, https://doi.org/10.1785/0120030259.

Roman, D.C., Neuberg, J, and Luckett, R.R., 2006, Assessing the likelihood of volcanic eruption through analysis of volcano-tectonic earthquake fault-plane solutions: Earth and Planetary Science Letters, v. 248, no. 1–2, p. 244–252, https://doi.org/10.1016/j.epsl.2006.05.029.

Roman, D.C., Soldati, A., Dingwell, D.B., Houghton, B.F., and Shiro, B.R., 2021, Earthquakes indicated magma viscosity during Kīlauea's 2018 eruption: Nature, v. 592, p. 237–241, https://doi.org/10.1038/s41586-021-03400-x.

Sánchez, J.J., Wyss, M., and McNutt, S.R., 2004, Temporal-spatial variations of stress at Redoubt Volcano, Alaska, inferred from inversion of fault plane solutions: Journal of Volcanology and Geothermal Research, v. 130, no. 1–2, p. 1–30, https://doi.org/10.1016/S0377-0273(03)00224-5.

Shelly, D.R., Hill, D.P., Massin, F., Farrell, J., Smith, R.B., and Taira, T., 2013, A fluid-driven earthquake swarm on the margin of the Yellowstone caldera: Journal of Geophysical Research, Solid Earth, v. 118, no. 9, p. 4872–4886, https://doi.org/10.1002/jgrb.50362.

Shelly, D.R., and Thelen, W.A., 2019, Anatomy of a caldera collapse—Kīlauea 2018 summit seismicity sequence in high resolution: Geophysical Research Letters, v. 46, no. 24, p. 14395–14403, https://doi.org/10.1029/2019GL085636.

Snoke, J.A., 2003, FOMEC—FOCal MEChanism determinations: International Geophysics, v. 81, no. B, p. 1629–1630, https://doi.org/10.1016/S0074-6142(03)80291-7.

Soubestre, J., Seydoux, L., Shapiro, N.M., de Rosny, J., Droznin, D.V., Droznina, S.Y., Senyukov, S.L., and Gordeev, E.I., 2019, Depth migration of seismovolcanic tremor sources below the Klyuchevskoy volcanic group (Kamchatka) determined from a network-based analysis: Geophysical Research Letters, v. 46, no. 14, p. 8018–8030, https://doi.org/10.1029/2019GL083465.

Taisne, B., Brenguier, F., Shapiro, N.M., and Ferrazzini, V., 2011, Imaging the dynamics of magma propagation using radiated seismic intensity: Geophysical Research Letters, Solid Earth, v. 38, no. 4, https://doi.org/10.1029/2010GL046068.

Takagi, N., Kaneshima, S., Kawakatsu, H., Yamamoto, M., Sudo, Y., Ohkura, T., Yoshikawa, S., and Mori, T., 2006, Apparent migration of tremor source synchronized with the change in the tremor amplitude observed at Aso Volcano, Japan: Journal of Volcanology and Geothermal Research, v. 154, no. 3–4, p. 181–200, https://doi.org/10.1016/j.jvolgeores.2006.02.001.

Tan, D., Fee, D., Hotovec-Ellis, A.J., Pesicek, J.D., Haney, M.M., Power, J.A., and Girona, T., 2023, Volcanic earthquake catalog enhancement using integrated detection, matched-filtering, and relocation tools: Frontiers in Earth Science, v. 11, article no. 1158442, https://doi.org/10.3389/feart.2023.1158442.

Thelen, W.A., 2014, Seismic instrumentation plan for the Hawaiian Volcano Observatory: U.S. Geological Survey Scientific Investigations Report 2014–5179, 43 p., https://doi.org/10.3133/sir20145179.

Thelen, W.A., Lyons, J.J., Iezzi, A.M., and Moran, S.C., 2024, Monitoring lahars and debris flows, chap. H *of* Flinders, A.F., Lowenstern, J.B., Coombs, M.L., and Poland, M.P., eds., Recommended capabilities and instrumentation for volcano monitoring in the Unites States: U.S. Geological Survey Scientific Investigations Report 2024–5062–H, 6 p., https://doi.org/10.3133/sir20245062H.

U.S. Geological Survey, 2017, Advanced National Seismic System—Current status, development opportunities, and priorities for 2017–2027 (ver.1.1, July 2017): U.S. Geological Survey Circular 1429, 32 p., https://doi.org/10.3133/cir1429.

U.S. Geological Survey Earthquake Hazards Program, 2019, Advanced National Seismic System Implementation Standards and Procedures (ver. 2.0): U.S. Geological Survey web page, accessed April 26, 2024, at https://www.usgs.gov/media/files/anss-implementation-standards.

Vinciguerra, S., 2002, Damage mechanics preceding the September–October 1989 flank eruption at Mount Etna Volcano inferred by seismic scaling exponents: Journal of Volcanology and Geothermal Research, v. 113, no. 3–4, p. 391–397, https://doi.org/10.1016/S0377-0273(01)00274-8.

White, R., 1996, Precursory deep long-period earthquakes at Mount Pinatubo—Spatio-temporal link to a basalt trigger, *in* Newhall, C.S., and Punongbayan, S., eds., Fire and mud—Eruptions and lahars of Mount Pinatubo, Philippines: Seattle, University of Washington Press, p. 307–327.

Wilding, J.D., Zhu, W., Ross, Z.E., and Jackson, J.M., 2022, The magmatic web beneath Hawai'i: Science, v. 379, no. 6631, p. 462–468, https://doi.org/10.1126/science.ade5755.

Zhu, W., and Beroza, G.C., 2019, PhaseNet—A deep-neural-network-based seismic arrival-time picking method: Geophysical Journal International, v. 216, no. 1, p. 261–273, https://doi.org/10.1093/gji/ggy423.

Moffett Field Publishing Service Center, California
Manuscript approved July 10, 2024
Edited by Linda Rogers and Monica Erdman
Layout and design by Cory Hurd

Thelan and others—**Seismic Techniques and Suggested Instrumentation to Monitor Volcanoes**—Scientific Investigations Report 2024–5062–B

ISSN 2328-031X (print)
ISSN 2328-0328 (online)
https://doi.org/10.3133/sir20245062B